THE JOURNAL OF BIOLOGICAL CHEMISTRY VOL. 284, NO. 30, pp. 20034–20040, July 24, 2009

Stabilization of the *E** Form Turns Thrombin into an Anticoagulant*

Received for publication, April 23, 2009, and in revised form, May 14, 2009 Published, JBC Papers in Press, May 27, 2009, DOI 10.1074/jbc.M109.012344

Alaji Bah, Christopher J. Carrell, Zhiwei Chen, Prafull S. Gandhi, and Enrico Di Cera[1]

From the Department of Biochemistry and Molecular Biophysics, Washington University School of Medicine, St. Louis, Missouri 63110

Previous studies have shown that deletion of nine residues in the autolysis loop of thrombin produces a mutant with an anticoagulant propensity of potential clinical relevance, but the molecular origin of the effect has remained unresolved. The x-ray crystal structure of this mutant solved in the free form at 1.55 Å resolution reveals an inactive conformation that is practically identical (root mean square deviation of 0.154 Å) to the recently identified *E form. The side chain of Trp^{215} collapses into the active site by shifting >10 Å from its position in the active *E* form, and the oxyanion hole is disrupted by a flip of the Glu^{192}–Gly^{193} peptide bond. This finding confirms the existence of the inactive form *E** in essentially the same incarnation as first identified in the structure of the thrombin mutant D102N. In addition, it demonstrates that the anticoagulant profile often caused by a mutation of the thrombin scaffold finds its likely molecular origin in the stabilization of the inactive *E** form that is selectively shifted to the active *E* form upon thrombomodulin and protein C binding.**

Serine proteases of the trypsin family are responsible for digestion, blood coagulation, fibrinolysis, development, fertilization, apoptosis, and immunity (1). Activation of the protease requires the transition from a zymogen form (2) and formation of an ion pair between the newly formed amino terminus of the catalytic chain and the side chain of the highly conserved residue Asp^{194} (chymotrypsinogen numbering) next to the catalytic Ser^{195}. This ensures substrate access to the active site and proper formation of the oxyanion hole contributed by the backbone N atoms of Ser^{195} and Gly^{193} (3). The zymogen → protease conversion is classically associated with the onset of catalytic activity (3, 4) and provides a useful paradigm for understanding key features of protease function and regulation.

Recent kinetic (5) and structural (6, 7) studies of thrombin, the key protease in the blood coagulation cascade (8), have drawn attention to a significant plasticity of the trypsin fold that impacts the function of the enzyme in a decisive manner. The active form of the protease, *E*, coexists with an inactive form, *E**, that is distinct from the zymogen conformation (9). The *E** form features a collapse of the 215–217 β-strand into the active site and a flip of the peptide bond between residues Glu^{192} and Gly^{193} that disrupts the oxyanion hole. Importantly, the ion pair between Ile^{16} and Asp^{194} remains intact, suggesting that *E** is not equivalent to the zymogen form of the protease and that the *E**-*E* equilibrium is established after the conversion from the zymogen form has taken place. Indeed, existing structures of the zymogen forms of trypsin (10), chymotrypsin (11), and chymase (12) feature a broken Ile^{16}–Asp^{194} ion pair but no collapse of the 215–217 β-strand. Stopped-flow experiments show that the *E**-*E* conversion takes place on a time scale of <10 ms (5), as opposed to the much longer (100–1000 ms) time scale required for the zymogen-protease conversion (13, 14).

The *E** form is not a peculiarity of thrombin. The collapse of the 215–217 β-strand into the active site is observed in the inactive form of αI-tryptase (15), the high temperature requirement-like protease (16), complement factor D (17), granzyme K (18), hepatocyte growth factor activator (19), prostate kallikrein (20), and prostasin (21). A disrupted oxyanion hole is observed in complement factor B (22) and the arterivirus protease Nsp4 (23). The most likely explanation for the widespread occurrence of inactive conformations of trypsin-like proteases is that the *E**-*E* equilibrium is a basic property of the trypsin fold that fine tunes activity and specificity once the zymogen → protease conversion has taken place (9).

The new paradigm established by the *E**-*E* equilibrium has obvious physiological relevance. In the case of complement factors, kallikreins, tryptase, and some coagulation factors must be kept to a minimum until binding of a trigger factor ensues. Stabilization of *E** may afford a resting state of the protease waiting for action, as seen for other systems (24–28). For example, factor B is mostly inactive until binding of complement factor C3 unleashes catalytic activity at the site where amplification of C3 activation is most needed prior to formation of the membrane attack complex (29). Indeed, the crystal structure of factor B reveals a conformation with the oxyanion hole disrupted by a flip of the 192–193 peptide bond (22), as observed in the *E** form of thrombin (6, 7).

The allosteric equilibrium as shown in Scheme 1,

$$E^* \underset{k_{-1}}{\overset{k_1}{\rightleftharpoons}} E$$

SCHEME 1

* This work was supported, in whole or in part, by National Institutes of Health Grants HL49413, HL58141, and HL73813 (to E. D. C.).

The atomic coordinates and structure factors (code 3gic) have been deposited in the Protein Data Bank, Research Collaboratory for Structural Bioinformatics, Rutgers University, New Brunswick, NJ (http://www.rcsb.org/).

[1] To whom correspondence should be addressed: Dept. of Biochemistry and Molecular Biophysics, Washington University School of Medicine, Box 8231, St. Louis, MO 63110. Tel.: 314-362-4185; Fax: 314-362-4311; E-mail: enrico@wustl.edu.

involves the rates for the $E^* \rightarrow E$ transition, k_1, and backward, k_{-1}, that define the equilibrium constant $r = k_{-1}/k_1 = [E^*]/[E]$ (5). The value of k_{cat}/K_m for an enzyme undergoing the E^*-E equilibrium is as shown in Equation 1 (30),

$$\frac{k_{cat}}{K_m} = s = \frac{s_E}{1 + r} \quad \text{(Eq. 1)}$$

where s_E is the value of s for the E form, and obviously $s_{E^*} = 0$. Likewise, the binding of an inhibitor to the enzyme undergoing the E^*-E equilibrium is shown in Equation 2,

$$K = \frac{K_E}{1 + r} \quad \text{(Eq. 2)}$$

where K_E is the value of the equilibrium association constant K for the E form, and $K_{E^*} = 0$. As the value of r increases upon stabilization of E^*, the values of s and K in Equations 1 and 2 decrease without limits. Hence, stabilization of E^* has the potential to completely abrogate substrate hydrolysis ($s \rightarrow 0$) or inhibitor binding ($K \rightarrow 0$). However, binding of a suitable cofactor could restore activity by triggering the $E^* \rightarrow E$ transition. This suggests a simple explanation for the anticoagulant profile observed in a number of thrombin mutants that have poor activity toward all physiological substrates but retain activity toward the anticoagulant protein C in the presence of the cofactor thrombomodulin (31–34). Here we report evidence that stabilization of E^* provides a molecular mechanism to turn thrombin into an anticoagulant.

MATERIALS AND METHODS

The human thrombin mutant Δ146–149e was constructed, expressed, and purified to homogeneity as reported elsewhere (32, 35, 36), using the QuikChange site-directed mutagenesis kit from Stratagene (La Jolla, CA) in an HPC4-modified pNUT expression vector containing the human prethrombin-1 gene. Values of $s = k_{cat}/K_m$ for the hydrolysis of the chromogenic substrates H-D-Phe-Gly-Arg-*p*-nitroanilide, H-D-Phe-Pro-Phe-*p*-nitroanilide, H-D-Phe-Pro-Lys-*p*-nitroanilide, and H-D-Phe-Pro-Arg-*p*-nitroanilide (FPR),[2] the release of fibrinopeptide A from fibrinogen, cleavage of the protease-activated receptors PAR1, PAR3, and PAR4, and activation of protein C in the absence or presence of 100 nM thrombomodulin and 5 mM $CaCl_2$ were determined as reported elsewhere (32, 37, 38) under physiological experimental conditions of 5 mM Tris, 0.1% PEG8000, 145 mM NaCl, pH 7.4, at 37 °C.

Binding of the active site inhibitor argatroban (39) was studied directly by isothermal titration calorimetry under experimental conditions of 5 mM Tris, 0.1% PEG8000, 145 mM NaCl, pH 7.4, at 37 °C, using an iTC200 calorimeter (MicroCal Inc. Northampton, MA) with the sample cell containing thrombin and the syringe injecting argatroban. The sample volume for iTC200 is 204.6 μl and the total volume of injected ligand is 39.7 μl. The thermal equilibration step at 37 °C, was followed by an initial 60-s delay step and subsequently an initial 0.2-μl injection. Typically, 19 serial injections of 2 μl and 1 last injection of 1.5 μl of ligand were performed at an interval of 180 s. The stirring speed was maintained at 1000 rpm, and the reference power was kept constant at 5 μcal/s. The heat associated with each injection of ligand was integrated and plotted against the molar ratio of ligand to macromolecule. Thermodynamic parameters were extracted from a curve fit to the data using the software (Origin 7.0) provided by MicroCal according to a one-site binding model. Experiments were performed in triplicate with excellent reproducibility (<10% variation in thermodynamic parameters).

Crystals of human thrombin Δ146–149e were obtained using the hanging drop vapor-diffusion method. A solution of Δ146–149e (8 mg/ml in 1 μl) in 50 mM NaCl, 20 mM Tris, pH 7.5, was mixed with an equal volume reservoir solution containing 20% PEG20000 and 100 mM Tris, pH 8.5, at 25 °C. Crystals were tetragonal, space group $P4_3$, with unit cell parameters $a = b = 58.2$ Å, $c = 119.6$ Å, and contained one molecule in the asymmetric unit. Crystals were flash-frozen in liquid nitrogen after soaking in artificial mother liquor containing 15% (v/v) glycerol. X-ray diffraction data were recorded on an ADSC Quantum 315 CCD at beamline 14-BM-C at BIOCARS (Argonne, IL). One pass of 150° with steps of 0.5° was collected and processed to 1.55 Å resolution. Integration and scaling of diffraction data were carried out with the HKL-2000 package (40). The structure was solved by molecular replacement using the CCP4 suite (41) and Protein Data Bank accession code 2GP9 (7) as a search model. Rounds of positional and isotropic temperature factor refinement in REFMAC (42) were alternated with model building in COOT (43). After most of the model was found, TLS tensors modeling rigid-body anisotropic temperature factors were calculated and applied to the model using REFMAC. This was alternated with more model building in COOT until the final model was produced. Ramachandran plots were calculated using PROCHECK (44). Statistics for data collection and refinement are summarized in Table 1. Coordinates of the structure of the human thrombin mutant Δ146–149e have been deposited to the Protein Data Bank (accession code 3GIC).

RESULTS

Once generated in the blood from its inactive precursor prothrombin, thrombin acts as a procoagulant when it converts fibrinogen into an insoluble fibrin clot (45) and acts as a prothrombotic when it cleaves protease-activated receptors (PARs) (46, 47). However, upon interaction with the endothelial cell receptor thrombomodulin, thrombin loses both procoagulant and prothrombotic functions and increases its activity >1,000-fold toward the anticoagulant protein C (48). A thrombin mutant stabilized in the E^* form would have little or no activity toward physiological substrates. If this mutant could be converted to the E form upon binding of thrombomodulin, then a selective anticoagulant response would be elicited upon activation of protein C in the vascular endothelium where thrombomodulin is present.

The mutant Δ146–149e carries a deletion of the nine residues ^{146}ETWTANVGK^{149e} in the autolysis loop and was originally constructed to assess the role of this highly flexi-

[2] The abbreviations used are: FPR, H-D-Phe-Pro-Arg-*p*-nitroanilide; r.m.s.d., root mean square deviation; PC, protein C; TM, thrombomodulin; PAR, protease-activated receptor.

TABLE 1

Crystallographic data for the thrombin mutant Δ146–149e (Protein Data Bank code 3GIC)

Data collection	
Wavelength	0.9 Å
Space group	$P4_3$
Unit cell dimension	$a = b = 58.23$, $c = 119.56$ Å
Molecules/asymmetric unit	1
Resolution range	40.0–1.55 Å
Observations	220,618
Unique observations	54,240
Completeness	94.3% (76.1%)
R_{sym} (%)	3.7% (27.9%)
$I/\sigma(I)$	27.7 (2.3)
Refinement	
Resolution	40.0–1.55 Å
$\|F\|/\sigma(\|F\|)$	>0
R_{cryst}, R_{free}	0.188, 0.224
Reflections (working/test)	51,479/2747
Protein atoms	2295
Solvent molecules	257
r.m.s.d. bond lengths[a]	0.012 Å
r.m.s.d. angles[a]	1.4°
r.m.s.d. ΔB (Å^2) (mm/ms/ss)[b]	0.86/0.67/2.21
⟨B⟩ protein	18.6 Å^2
⟨B⟩ solvent	28.6 Å^2
Ramachandran plot	
Most favored	98.3%
Generously allowed	1.3%
Disallowed	0.4%

[a] Root mean square deviations from ideal bond lengths and angles and r.m.s.d. values in B-factors of bonded atoms are shown.

[b] mm indicates main chain-main chain; ms indicates main chain-side chain; and ss indicates side chain-side chain.

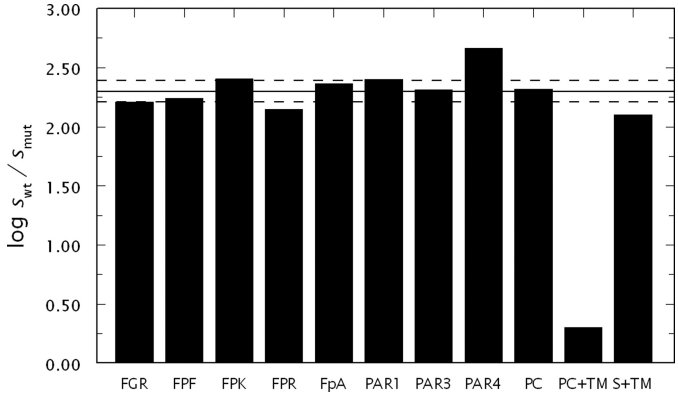

FIGURE 1. **Functional properties of the thrombin mutant Δ146–149e.** Shown are the values of $s = k_{cat}/K_m$ for the hydrolysis of chromogenic substrates H-D-Phe-Gly-Arg-*p*-nitroanilide (*FGR*), H-D-Phe-Pro-Phe-*p*-nitroanilide (*FPF*), H-D-Phe-Pro-Lys-*p*-nitroanilide (*FPK*), and FPR, fibrinogen (*FpA*), PAR1, PAR3, PAR4, protein C (*PC*), and protein C (*PC+TM*) or FPR (*S+TM*) in the presence of 100 nM thrombomodulin and 5 mM $CaCl_2$ for wild-type (s_{wt}) relative to the thrombin mutant Δ146–149e (s_{mut}). All substrates, except PAR4, experience a loss of activity that equals 2.30 log units (*solid line*) with a standard deviation of 0.09 log units (*broken lines*). This supports perturbation of the *E*-E* equilibrium in favor of the inactive form *E** (see Equations 1 and 3 in the text). The larger loss for PAR4 (>4 S.D. compared with the other substrates) is likely due to direct interaction of the substrate with residues of the autolysis loop (55) that are missing in the Δ146–149e mutant. In the presence of thrombomodulin, the mutant experiences only a 2-fold drop in activity toward protein C compared with wild type. However, thrombomodulin binding alone does not restore activity toward the chromogenic substrate FPR. Experimental conditions are as follows: 5 mM Tris, 0.1% PEG8000, 145 mM NaCl, pH 7.4, at 37 °C. The values of s_{wt} are as follows: 0.52 ± 0.05 μM^{-1} s^{-1} H-D-Phe-Gly-Arg-*p*-nitroanilide (*FGR*), 0.28 ± 0.03 μM^{-1} s^{-1} H-D-Phe-Pro-Gly-*p*-nitroanilide (*FGF*), 4.2 ± 0.2 $\mu M^{-1}s^{-1}$ H-D-Phe-Pro-Gly-*p*-nitroanilide (*FGK*), 37 ± 1 μM^{-1} s^{-1} H-D-Phe-Pro-Arg-*p*-nitroanilide (*FPR*), 17 ± 1 μM^{-1} s^{-1} fibrinogen (*FpA*), 39 ± 1 $\mu M^{-1}s^{-1}$ PAR1, 0.35 ± 0.02 μM^{-1} s^{-1} PAR3, 0.34 ± 0.01 μM^{-1} s^{-1} PAR4, 59 ± 3 M^{-1} s^{-1} PC, 0.22 ± 0.01 $\mu M^{-1}s^{-1}$ PC+TM, 64 ± 2 $\mu M^{-1}s^{-1}$ S+TM.

ble domain in thrombin function (49). The sequence ^{149a}ANVGK^{149e} is not present in trypsin and chymotrypsin and can be deleted without functional consequences (49). Also, swapping the entire ^{146}ETWTANVGK^{149e} sequence of thrombin with the ^{146}SSGT^{149} sequence of trypsin (50) or deleting the ^{146}ETW^{148} sequence (51) produces perturbations of function that are recapitulated by the single mutations E146A and R221aA (32, 35). Residue Glu^{146} makes an important ion pair interaction with Arg^{221a} in the adjacent 220-loop in the *E* form but not in the *E** form (6, 7, 35). The entire autolysis loop likely participates in the long range communication seen in the *E*-E* equilibrium (6) between the 220-loop, the active site, and exosite I where thrombomodulin binds (8). Deletion of the entire sequence ^{146}ETWTANVGK^{149e} in the Δ146–149e mutant causes a significant loss of activity toward chromogenic and physiological substrates, but binding of thrombomodulin almost completely restores activity toward the anticoagulant protein C (Fig. 1). Importantly, thrombomodulin has only a modest effect on the hydrolysis of a chromogenic substrate (Fig. 1), as already documented for other anticoagulant thrombin mutants (52) and wild type (53). These properties suggest that the Δ146–149e mutation shifts the *E*-E* equilibrium of thrombin in favor of *E**, and thrombomodulin in complex with protein C can switch the mutant back into the active conformation *E*.

Evidence that the thrombin mutant Δ146–149e is stabilized in the *E** form in solution comes from inspection of the values of k_{cat}/K_m for chromogenic and natural substrates. The data in Fig. 1 reveal a remarkable similarity in the loss of activity toward fibrinogen, PAR1, PAR3, and protein C for the Δ146–149e mutant compared with wild type. Likewise, a comparable loss of activity is observed toward several chromogenic substrates bearing replacements at the P1 or P2 positions (54). On the average, the loss is about 200-fold. For a mutation that selectively shifts the *E*-E* equilibrium in favor of *E**, without introducing additional effects on substrate or inhibitor recognition, the values of *s* and *K* in Equations 1–2 must decrease by the same amount. Specifically, the ratio shown in Equation 3 between the wild-type (WT) and mutant values of *s* and *K* must be the same for all substrates and inhibitors.

$$\frac{s_{WT}}{s_{mut}} = \frac{K_{WT}}{K_{mut}} = \frac{1 + r_{mut}}{1 + r_{WT}} \qquad \text{(Eq. 3)}$$

The data in Fig. 1 are consistent with the prediction from Equation 3. Perturbation of PAR4 recognition is significantly more pronounced compared with all other substrates, but this is consistent with the direct interactions that this substrate makes with residues of the autolysis loop (55). Further support for stabilization of *E** in the Δ146–149e mutant comes from calorimetric measurements of the binding of the inhibitor argatroban (39) to the active site. The value of *K* (see Equation 2) drops 135-fold in the mutant compared with wild type (Fig. 2), as expected from Equation 3.

Addition of thrombomodulin restores activity of the mutant toward protein C (Fig. 1), indicating that although the mutation stabilizes *E**, the active form *E* is still present in solution and can be populated for protein C activation in the presence of cofac-

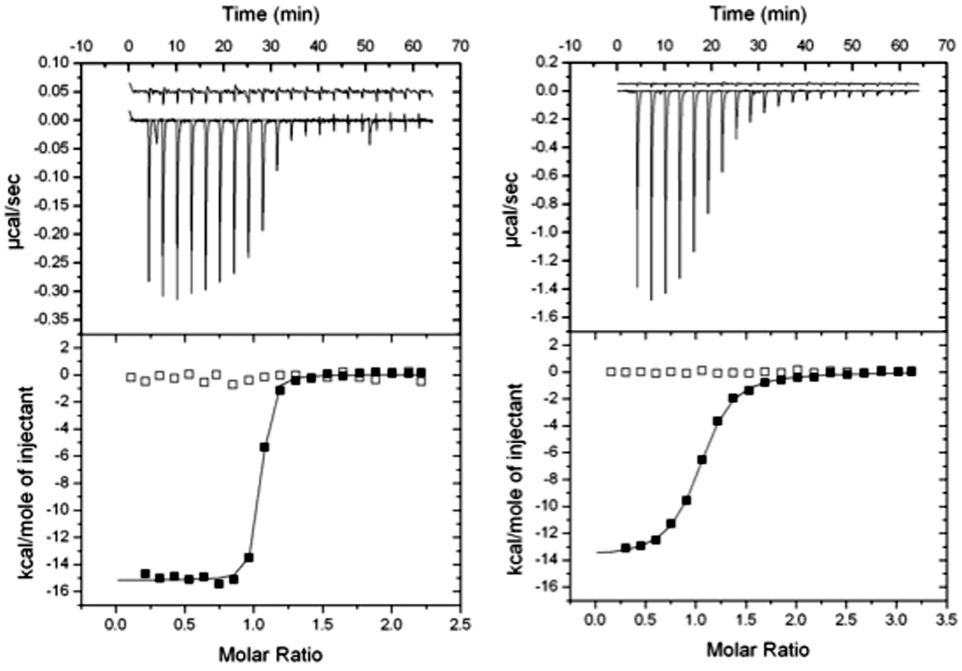

FIGURE 2. **Argatroban binding to thrombin wild type (*left*) and Δ146–149e (*right*) measured by isothermal titration calorimetry.** The *top panel* shows the heat exchanged in each individual titration for the thrombin sample (*bottom trace*) and the argatroban buffer control (*top trace*). The *bottom panel* is the integration of the data to yield the overall heat exchanged as a function of the ligand/protein molar ratio. Experimental conditions are 5 mM Tris, 0.1% polyethylene glycol, 145 mM NaCl, pH 7.4, 37 °C. The enzyme and argatroban concentrations are as follows: 13.44 and 140 μM (thrombin wild type); 52.5 and 777 μM (Δ146–149e). Titration curves were fit using the Origin software of the iTC200, with best fit parameter values as follows: thrombin wild type, $K = 1.0 \pm 0.1\ 10^8\ M^{-1}$, $\Delta G = -11.3 \pm 0.1$ kcal/mol, $\Delta H = -15.2 \pm 0.1$ kcal/mol, and $T\Delta S = -3.9 \pm 0.1$ kcal/mol; Δ146–149e, $K = 7.4 \pm 0.4\ 10^5\ M^{-1}$, $\Delta G = -8.3 \pm 0.1$ kcal/mol, $\Delta H = -13.8 \pm 0.1$ kcal/mol, and $T\Delta S = -5.5 \pm 0.1$ kcal/mol. The value of the stoichiometric constant *N* was 1.01 ± 0.01 for thrombin wild type and the Δ146–149e mutant.

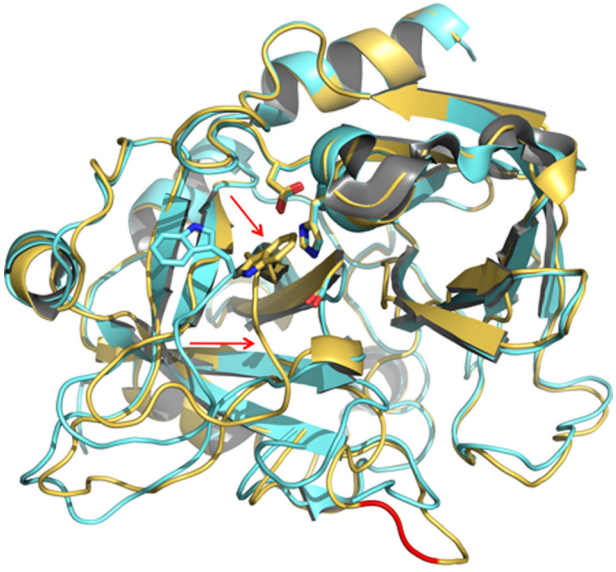

FIGURE 3. **Ribbon representation of the structure of the thrombin mutant Δ146–149e (*gold*) overlaid with the structure of thrombin in the *E* conformation (35) (*cyan*).** The newly formed peptide bond between Lys^{145} and Gly^{150} is indicated in *red* in the shortened autolysis loop of Δ146–149e (see also Fig. 4), and the loop in the *E* conformation is not visible between residues Trp^{148} and Lys^{149e}. The 215–217 β-strand in the mutant collapses into the primary specificity pocket (*red open arrowheads*), with the side chain of Trp^{215} (*stick model*) repositioned into the active site (residues of the catalytic triad His^{57}, Asp^{102}, and Ser^{195} shown as *stick models*) in hydrophobic interaction with Trp^{60d}, Tyr^{60a}, Leu^{99}, and His^{57}. This represents a drastic change (r.m.s.d. 0.384 Å) from the conformation of *E* where the side chain of Trp^{215} is positioned 10.5 Å away and leaves the active site accessible to substrate. The conformation of Δ146–149e is remarkably similar (r.m.s.d. 0.154 Å) to that of *E** determined recently (6, 7).

tor. Evidence that binding to exosite I, the major thrombin epitope for thrombomodulin recognition (56, 57), can convert *E** to *E* has been provided recently by the structure of the thrombin mutant D102N bound to a fragment of the platelet receptor PAR1 (6). Therefore, the thrombin mutant Δ146–149e likely functions as an allosteric switch stabilized into the inactive form *E** until the combined binding of thrombomodulin and protein C shifts *E** to *E* and restores activity.

To gain direct information on the conformational properties of the Δ146–149e mutant, its crystal structure was solved in the free form at 1.55 Å resolution. Consistent with the functional data, the mutant assumes a collapsed conformation that is practically identical (r.m.s.d. 0.154 Å) to the *E** form identified recently from the structure of the thrombin mutant D102N (6, 7). The Δ146–149e mutant folds in a self-inhibited conformation (Fig. 3) due to a collapse of the 215–217 β-strand into the active site that moves the indole ring of Trp^{215} >10 Å to engage the catalytic His^{57} on the opposite side of the active site cleft (Fig. 4). The drastic rearrangement of the 215–217 β-strand propagates the perturbation up to the peptide bond between Glu^{192} and Gly^{193} that is flipped relative to the conformation of the *E* form (7) and destroys the architecture of the oxyanion hole (Fig. 4). These significant structural changes occur away from the site of mutation in the autolysis loop, where the shortened sequence $^{144}LKGQ^{151}$ shows Lys^{145} connected directly to Gly^{150} (Fig. 4). Hence, the thrombin mutants D102N and Δ146–149e crystallize in the same *E** form, notwithstanding differences in sequence and crystallization conditions. The inactive form *E** is therefore a genuine conformation of thrombin accessible to the enzyme in addition to its active form *E* (9, 35). The *E** form is stabilized by mutations that compromise activity of the enzyme and is selectively converted to the active *E* form under suitable conditions.

DISCUSSION

The new paradigm emerged from analysis of recent crystal structures of trypsin-like proteases (6, 7, 15–23) supports the existence of the *E**-*E* equilibrium as a critical feature of the trypsin fold (9). This allosteric equilibrium explains several important aspects of protease biology. For proteases that are poorly active until interaction with a cofactor, as observed for some clotting and complement factors (29), the onset of catalytic activity can be attributed to the *E** ⟶ E conversion. The *E** form acts in this case as a resting state for the enzyme and a spring-loaded mechanism that can be turned on when required

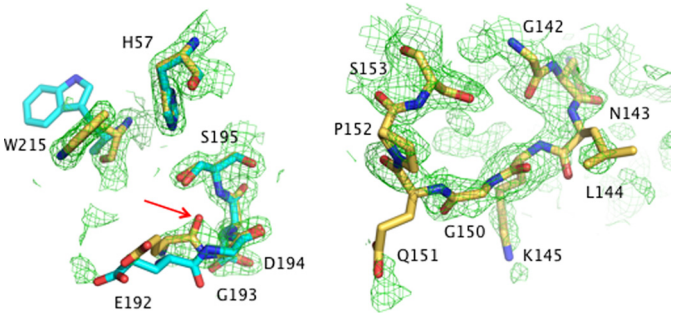

FIGURE 4. *Left,* details of the collapse of Trp^{215} into the active site and disruption of the oxyanion hole in the thrombin mutant Δ146–149e (CPK, *yellow*) are shown. The conformation of the same residues in the *E* form is shown by comparison (CPK, *cyan*). The peptide bond between Glu^{192} and Gly^{193} is flipped in the Δ146–149e mutant (*red open arrowhead*), as seen in the *E** form (6, 7, 9), causing disruption of the oxyanion hole contributed by the N atoms of Gly^{193} and Ser^{195}. The $2F_o - F_c$ electron density map (*green mesh*) is contoured at 2.0σ. *Right,* deletion of residues ^{146}ETWTANVGK^{149e} in the autolysis loop of the Δ146–149e mutant results in a new peptide bond connection between Lys^{145} and Gly^{150} (CPK, *yellow*). The autolysis loop is rarely seen in its entirety in thrombin structures, and considerable disorder remains in the mutant Δ146–149e where the sequence ^{144}LKGQ^{151} must be contoured at 0.5σ in the $2F_o - F_c$ electron density map (*green mesh*).

by the biological context. The *E*-E* equilibrium also provides context to interpret the effect of mutations associated with loss of biological activity in highly active proteases. In some cases, as documented by thrombin (8, 58), the molecular origin of the effect is unclear because the mutation does not affect residues in direct contact with substrate. Stabilization of *E** through molecular conduits not necessarily involved in substrate recognition may offer a plausible explanation.

The allosteric *E*-E* equilibrium has far reaching implications for protein engineering. Stabilization of *E** by selected mutations, coupled with a transition to *E* triggered by suitable cofactors, may result in expression of protease activity on demand in a biological context. Thrombin exists predominantly in the *E* form, which functions as an ensemble partitioned between Na^+-free and Na^+-bound conformations (5, 8) because of the extremely fast rates of binding and dissociation of Na^+ with the enzyme (59). However, a thrombin mutant stabilized in the *E** form that converts to *E* upon interaction with thrombomodulin and protein C would be an anticoagulant of potential clinical relevance. Such mutant would show little or no activity toward fibrinogen and PAR1 but would retain activity toward protein C. A number of thrombin mutants have been reported with an altered specificity that favors protein C activation over fibrinogen cleavage (31–34, 49, 60, 61). Among these mutants, E217K and W215A/E217A are effective as anticoagulants and antithrombotics in non-human primates (33, 34, 62, 63) and have been crystallized at 2.5–2.8 Å resolution (52, 64). The structures show a partial collapse of the 215–217 β-strand and disruption of the oxyanion hole that resembles the conformation of *E** (7). It is possible that these mutants are stabilized in an *E**-like form, but it is equally possible that the perturbed structures are the result of the mutations introduced at residues on the critical 215–217 β-strand. Substantial crystallographic packing interactions especially evident in the E217K mutant also bias the conformation, unlike the structures of the mutants D102N (7) and Δ146–149e reported here. Additional structural work is necessary to validate the collapsed conformations of E217K and W215A/E217A.

The mutant Δ146–149e was previously identified for its significant anticoagulant profile (49) and carries a deletion of nine residues in the highly disordered autolysis loop, whose role in the function of the enzyme remains elusive. Importantly, residues of the autolysis loop are separate from the 215–217 β-strand or the oxyanion hole that undergoes substantial rearrangement in the *E*-E* transition (6, 7). Yet the mutant Δ146–149e crystallizes in a collapsed conformation that is practically identical (r.m.s.d. 0.154 Å) to the *E** form identified recently (6, 7). This result is notable for two reasons. First, it confirms the existence of the inactive form *E** in essentially the same incarnation as first identified in the structure of the thrombin mutant D102N under different crystallization conditions. Second, it provides proof of principle that the anticoagulant profile often caused by a mutation of the thrombin scaffold finds its likely molecular origin into stabilization of the inactive *E** form. The mutant Δ146–149e was previously reported to feature reduced Na^+ affinity (49), which supports the conclusion that its active *E* form is essentially Na^+-free. This confirms the tenet that abrogation of the procoagulant effect of Na^+ (32, 65) is necessary to switch thrombin into an anticoagulant.

There is no contradiction between the modest effect of thrombomodulin on chromogenic substrate hydrolysis (Fig. 1) and structural evidence of the *E** to *E* transition upon exosite I binding (6). Crystallographic evidence that the D102N mutant assumes the *E** form when free and the *E* form when bound to exosite I does not imply an all-or-none distribution of *E** and *E* in solution. In fact, a significant fraction of D102N does exist in the *E* form in solution (7), but this conformation is not favored under the crystallization conditions so far explored (7). Thermodynamic principles (66, 67) establish that an allosteric effector can only shift the *E*-E* equilibrium in favor of *E* by an amount equal to the ratio of affinities of the two forms. Because exosite I, unlike the active site, is similarly accessible in the *E** and *E* form (6–8, 35), binding of thrombomodulin to the two forms cannot result in extreme perturbations of the *E*-E* equilibrium. Hence, when the equilibrium is shifted drastically in favor of *E**, as seen for the Δ146–149e mutant but not the D102N mutant, binding of thrombomodulin is insufficient to populate significantly the active form *E*. On the other hand, the combined action of protein C and thrombomodulin may have a more profound effect on the *E*-E* equilibrium by accessing additional regions of the thrombin surface beyond exosite I (57), thereby ensuring almost complete restoration of activity.

Elucidation of the molecular mechanism underscoring the anticoagulant profile of thrombin mutants like Δ146–149e provides new impetus to the effort of rationally engineering thrombin mutants with exclusive activity toward protein C for clinical applications. The molecular underpinnings of the *E*-E* equilibrium have been revealed by structural biology (6), along with precise targets for mutagenesis aimed at stabilizing the *E** form. An exclusive protein C activator would have several advantages compared with the direct administration of activated protein C currently marketed for the treatment of sepsis (68). Activated protein C acts as an anticoagulant when it inactivates clotting factor Va with the assistance of the cofactor

protein S and as a cytoprotective agent when it cleaves PAR1 on the surface of endothelial cells with the assistance of endothelial protein C receptor (69). Importantly, activated protein C generated *in situ* with the anticoagulant thrombin mutant W215A/E217A offers cytoprotective advantages over activated protein C administered to the circulation (70). Furthermore, the thrombin mutant W215A/E217A acts as a potent antithrombotic by blocking the interaction of von Willebrand factor with the platelet receptor GpIb (71), a property of which activated protein C is naturally devoid and that challenges the efficacy of low molecular weight heparins (63). These intriguing properties of the mutant W215A/E217A, its well established potency as an anticoagulant in non-human primates (62, 63) and the current elucidation of the role of E^* in switching thrombin into an anticoagulant, will facilitate the rational engineering of a thrombin mutant with exclusive activity toward protein C.

REFERENCES

1. Page, M. J., and Di Cera, E. (2008) *Cell. Mol. Life Sci.* **65,** 1220–1236
2. Bode, W., and Huber, R. (1976) *FEBS Lett.* **68,** 231–236
3. Hedstrom, L. (2002) *Chem. Rev.* **102,** 4501–4524
4. Bode, W., Schwager, P., and Huber, R. (1978) *J. Mol. Biol.* **118,** 99–112
5. Bah, A., Garvey, L. C., Ge, J., and Di Cera, E. (2006) *J. Biol. Chem.* **281,** 40049–40056
6. Gandhi, P. S., Chen, Z., Mathews, F. S., and Di Cera, E. (2008) *Proc. Natl. Acad. Sci. U.S.A.* **105,** 1832–1837
7. Pineda, A. O., Chen, Z. W., Bah, A., Garvey, L. C., Mathews, F. S., and Di Cera, E. (2006) *J. Biol. Chem.* **281,** 32922–32928
8. Di Cera, E. (2008) *Mol. Aspects Med.* **29,** 203–254
9. Di Cera, E. (2009) *IUBMB Life* **61,** 510–515
10. Fehlhammer, H., Bode, W., and Huber, R. (1977) *J. Mol. Biol.* **111,** 415–438
11. Wang, D., Bode, W., and Huber, R. (1985) *J. Mol. Biol.* **185,** 595–624
12. Reiling, K. K., Krucinski, J., Miercke, L. J., Raymond, W. W., Caughey, G. H., and Stroud, R. M. (2003) *Biochemistry* **42,** 2616–2624
13. Fersht, A. R. (1972) *J. Mol. Biol.* **64,** 497–509
14. Fersht, A. R., and Requena, Y. (1971) *J. Mol. Biol.* **60,** 279–290
15. Rohr, K. B., Selwood, T., Marquardt, U., Huber, R., Schechter, N. M., Bode, W., and Than, M. E. (2006) *J. Mol. Biol.* **357,** 195–209
16. Krojer, T., Garrido-Franco, M., Huber, R., Ehrmann, M., and Clausen, T. (2002) *Nature* **416,** 455–459
17. Jing, H., Babu, Y. S., Moore, D., Kilpatrick, J. M., Liu, X. Y., Volanakis, J. E., and Narayana, S. V. (1998) *J. Mol. Biol.* **282,** 1061–1081
18. Hink-Schauer, C., Estébanez-Perpiñá, E., Wilharm, E., Fuentes-Prior, P., Klinkert, W., Bode, W., and Jenne, D. E. (2002) *J. Biol. Chem.* **277,** 50923–50933
19. Shia, S., Stamos, J., Kirchhofer, D., Fan, B., Wu, J., Corpuz, R. T., Santell, L., Lazarus, R. A., and Eigenbrot, C. (2005) *J. Mol. Biol.* **346,** 1335–1349
20. Carvalho, A. L., Sanz, L., Barettino, D., Romero, A., Calvete, J. J., and Romão, M. J. (2002) *J. Mol. Biol.* **322,** 325–337
21. Rickert, K. W., Kelley, P., Byrne, N. J., Diehl, R. E., Hall, D. L., Montalvo, A. M., Reid, J. C., Shipman, J. M., Thomas, B. W., Munshi, S. K., Darke, P. L., and Su, H. P. (2008) *J. Biol. Chem.* **283,** 34864–34872
22. Ponnuraj, K., Xu, Y., Macon, K., Moore, D., Volanakis, J. E., and Narayana, S. V. (2004) *Mol. Cell* **14,** 17–28
23. Barrette-Ng, I. H., Ng, K. K., Mark, B. L., Van Aken, D., Cherney, M. M., Garen, C., Kolodenko, Y., Gorbalenya, A. E., Snijder, E. J., and James, M. N. (2002) *J. Biol. Chem.* **277,** 39960–39966
24. Eisenmesser, E. Z., Bosco, D. A., Akke, M., and Kern, D. (2002) *Science* **295,** 1520–1523
25. Lu, H. P., Xun, L., and Xie, X. S. (1998) *Science* **282,** 1877–1882
26. Sytina, O. A., Heyes, D. J., Hunter, C. N., Alexandre, M. T., van Stokkum, I. H., van Grondelle, R., and Groot, M. L. (2008) *Nature* **456,** 1001–1004
27. Erlandson, K. J., Miller, S. B., Nam, Y., Osborne, A. R., Zimmer, J., and Rapoport, T. A. (2008) *Nature* **455,** 984–987
28. Zimmer, J., Nam, Y., and Rapoport, T. A. (2008) *Nature* **455,** 936–943
29. Gros, P., Milder, F. J., and Janssen, B. J. (2008) *Nat. Rev. Immunol.* **8,** 48–58
30. Carrell, C. J., Bush, L. A., Mathews, F. S., and Di Cera, E. (2006) *Biophys. Chem.* **121,** 177–184
31. Cantwell, A. M., and Di Cera, E. (2000) *J. Biol. Chem.* **275,** 39827–39830
32. Dang, Q. D., Guinto, E. R., and di Cera, E. (1997) *Nat. Biotechnol.* **15,** 146–149
33. Gibbs, C. S., Coutré, S. E., Tsiang, M., Li, W. X., Jain, A. K., Dunn, K. E., Law, V. S., Mao, C. T., Matsumura, S. Y., Mejza, S. J., Paborsky, L. R., and Leung, L. L. (1995) *Nature* **378,** 413–416
34. Tsiang, M., Paborsky, L. R., Li, W. X., Jain, A. K., Mao, C. T., Dunn, K. E., Lee, D. W., Matsumura, S. Y., Matteucci, M. D., Coutré, S. E., Leung, L. L., and Gibbs, C. S. (1996) *Biochemistry* **35,** 16449–16457
35. Pineda, A. O., Carrell, C. J., Bush, L. A., Prasad, S., Caccia, S., Chen, Z. W., Mathews, F. S., and Di Cera, E. (2004) *J. Biol. Chem.* **279,** 31842–31853
36. Prasad, S., Wright, K. J., Banerjee Roy, D., Bush, L. A., Cantwell, A. M., and Di Cera, E. (2003) *Proc. Natl. Acad. Sci. U.S.A.* **100,** 13785–13790
37. Ayala, Y. M., Cantwell, A. M., Rose, T., Bush, L. A., Arosio, D., and Di Cera, E. (2001) *Proteins* **45,** 107–116
38. Vindigni, A., and Di Cera, E. (1996) *Biochemistry* **35,** 4417–4426
39. Tanaka, K. A., Gruber, A., Szlam, F., Bush, L. A., Hanson, S. R., and Di Cera, E. (2008) *Blood Coagul. Fibrinolysis* **19,** 465–468
40. Otwinowski, Z., and Minor, W. (1997) *Methods Enzymol.* **276,** 307–326
41. Bailey, S. (1994) *Acta Crystallogr. D Biol. Crystallogr.* **50,** 760–763
42. Murshudov, G. N., Vagin, A. A., and Dodson, E. J. (1997) *Acta Crystallogr. D Biol. Crystallogr.* **53,** 240–255
43. Emsley, P., and Cowtan, K. (2004) *Acta Crystallogr. D Biol. Crystallogr.* **60,** 2126–2132
44. Morris, A. L., MacArthur, M. W., Hutchinson, E. G., and Thornton, J. M. (1992) *Proteins* **12,** 345–364
45. Spraggon, G., Everse, S. J., and Doolittle, R. F. (1997) *Nature* **389,** 455–462
46. Coughlin, S. R. (2000) *Nature* **407,** 258–264
47. Coughlin, S. R. (2005) *J. Thromb. Haemost.* **3,** 1800–1814
48. Esmon, C. T. (2003) *Chest* **124,** 26S-32S
49. Dang, Q. D., Sabetta, M., and Di Cera, E. (1997) *J. Biol. Chem.* **272,** 19649–19651
50. DiBella, E. E., and Scheraga, H. A. (1996) *Biochemistry* **35,** 4427–4433
51. Le Bonniec, B. F., Guinto, E. R., and Esmon, C. T. (1992) *J. Biol. Chem.* **267,** 19341–19348
52. Pineda, A. O., Chen, Z. W., Caccia, S., Cantwell, A. M., Savvides, S. N., Waksman, G., Mathews, F. S., and Di Cera, E. (2004) *J. Biol. Chem.* **279,** 39824–39828
53. Vindigni, A., White, C. E., Komives, E. A., and Di Cera, E. (1997) *Biochemistry* **36,** 6674–6681
54. Vindigni, A., Dang, Q. D., and Di Cera, E. (1997) *Nat. Biotechnol.* **15,** 891–895
55. Bah, A., Chen, Z., Bush-Pelc, L. A., Mathews, F. S., and Di Cera, E. (2007) *Proc. Natl. Acad. Sci. U.S.A.* **104,** 11603–11608
56. Pineda, A. O., Cantwell, A. M., Bush, L. A., Rose, T., and Di Cera, E. (2002) *J. Biol. Chem.* **277,** 32015–32019
57. Xu, H., Bush, L. A., Pineda, A. O., Caccia, S., and Di Cera, E. (2005) *J. Biol. Chem.* **280,** 7956–7961
58. Papaconstantinou, M. E., Bah, A., and Di Cera, E. (2008) *Cell. Mol. Life Sci.* **65,** 1943–1947
59. Gianni, S., Ivarsson, Y., Bah, A., Bush-Pelc, L. A., and Di Cera, E. (2007) *Biophys. Chem.* **131,** 111–114
60. Griffin, J. H. (1995) *Nature* **378,** 337–338
61. Wu, Q. Y., Sheehan, J. P., Tsiang, M., Lentz, S. R., Birktoft, J. J., and Sadler, J. E. (1991) *Proc. Natl. Acad. Sci. U.S.A.* **88,** 6775–6779
62. Gruber, A., Cantwell, A. M., Di Cera, E., and Hanson, S. R. (2002) *J. Biol. Chem.* **277,** 27581–27584
63. Gruber, A., Marzec, U. M., Bush, L., Di Cera, E., Fernández, J. A., Berny, M. A., Tucker, E. I., McCarty, O. J., Griffin, J. H., and Hanson, S. R. (2007) *Blood* **109,** 3733–3740
64. Carter, W. J., Myles, T., Gibbs, C. S., Leung, L. L., and Huntington, J. A. (2004) *J. Biol. Chem.* **279,** 26387–26394
65. Dang, O. D., Vindigni, A., and Di Cera, E. (1995) *Proc. Natl. Acad. Sci.*

U.S.A. **92,** 5977–5981
66. Wyman, J., and Gill, S. J. (1990) *Binding and Linkage*, University Science Books, Mill Valley, CA
67. Di Cera, E. (1995) *Thermodynamic Theory of Site-Specific Binding Processes in Biological Macromolecules*, Cambridge University Press, Cambridge, UK
68. Levi, M. (2008) *Curr. Opin. Hematol.* **15,** 481–486
69. Riewald, M., Petrovan, R. J., Donner, A., Mueller, B. M., and Ruf, W. (2002) *Science* **296,** 1880–1882
70. Feistritzer, C., Schuepbach, R. A., Mosnier, L. O., Bush, L. A., Di Cera, E., Griffin, J. H., and Riewald, M. (2006) *J. Biol. Chem.* **281,** 20077–20084
71. Berny, M. A., White, T. C., Tucker, E. I., Bush-Pelc, L. A., Di Cera, E., Gruber, A., and McCarty, O. J. (2008) *Arterioscler. Thromb. Vasc. Biol.* **28,** 329–334